International Journal of Applied Engineering Research
ISSN 0973-4562 Volume 10, Number 3 (2015) pp. 5643-5661

http://www.ripublication.com

Investigations on the Performance of Small Hydro Power Plants with Deformation in Bulb Turbine Discharge Ring and Outer Distributor Cone

Dr.P.Sridharan[1] and Dr.N.Kuppuswamy[2]

1.Associate Professor/EIE, Maharaja Engineering College,Avinashi, Coimbatore, Tamilnadu-641654
2.Principal, Maharaja Engineering College,Avinashi,Coimbatore,Tamilnadu-641654
Email ID : sridharpsgtech@rediffmail.com

Abstract

Small Hydroelectric Power (SHP) development is increasingly undertaken all over the world, especially in the developing countries, because of their various merits, varied application, and flexibility of utilization. Increasing populations and new modern technologies necessitate massive amounts of electricity for creating, building and expanding. Cavitation occurs when the pressure at any point in the bulb turbine is reduced to the vapor pressure of the liquid. Under such conditions, vapor bubbles formed and then collapse, producing dynamic effects that leads to decreased efficiency and deformation of discharge ring hence the cavitation effects are fully avoided.

1 INTRODUCTION

In a liquid, if the pressure at any point reduces to its vapor pressure, the liquid boils and vaporization starts. If the liquid contains dissolved gases, they are liberated at such low pressures. A large number of small size bubbles of liquid vapor and liberated gas are thus formed. These are than carried by the flow. These bubbles upon reaching a zone of higher pressure condense and collapse abruptly. The surrounding liquid rushes to fill the space or cavity created by the bubbles collapse. The liquid is rushing from all the direction collides at the center of the cavity generating a pressure wave which travels almost at the velocity of sound thus giving rise to very high local pressures. If the bubbles collapse takes place at a solid boundary, it is subjected to these very high pressures. The boundary material may thus be stressed locally beyond its elastic limit, resulting ultimately in fatigue failure. Even if the bubbles collapse and the consequent formation of cavities do not occur at the solid boundary, the intense pressures are propagated to the boundary through the pressure wave which originates from the cavity center.

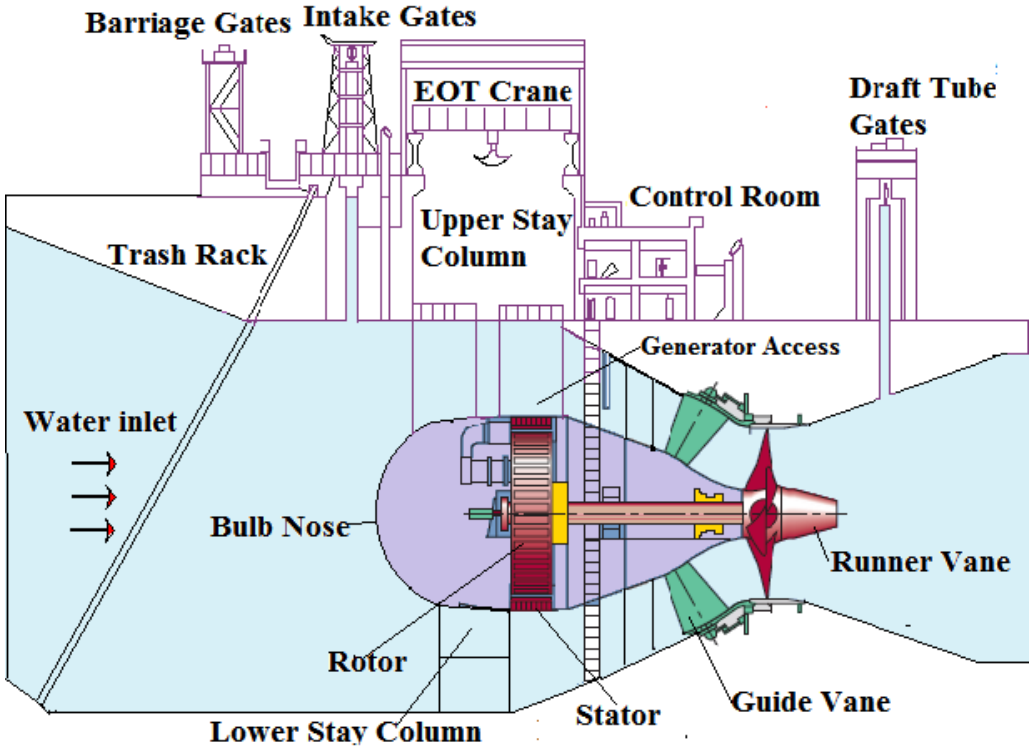

Figure 1 Outline of run of river power house

The layout of bulb turbine in a run of river powerhouse as shown in Figure 1. The run-of-river power stations utilize the irrigation demand left out in the river with chains of barrage power stations, such a way that the water flowing in the river is temporarily stored in each barrage and utilized for electrical power generation. In each barrage, the headrace water level is kept equal to the tailrace level of the previous powerhouse to avoid stagnation of tail race water in a chain of the power house.

This sequence of formation of vapor bubbles, their transport to zones of high pressure and subsequent collapse repeat itself many times in a second, the frequency depending directly on the velocity of the flow. These very high pressures acting repeatedly over the solid boundary as repeated hammer-blows at a high frequency, cause severe damage to the boundary surface. The surface becomes badly dented, and in some places its material appears to have been eroded by the liquid flow. This phenomenon is known as pitting, and the surface is said to have been pitted by the action of the flowing liquid. The material of the boundary surface ultimately fails by fatigue. The entire phenomenon characterized by the bubble formation and the subsequent collapse is known as the cavitation. There may be considerable noise and vibrations associated with the cavitating flow. The efficiency of the system also decreases on account of reduced flow-area due to the space occupied by the bubbles as shown in Figure 2.

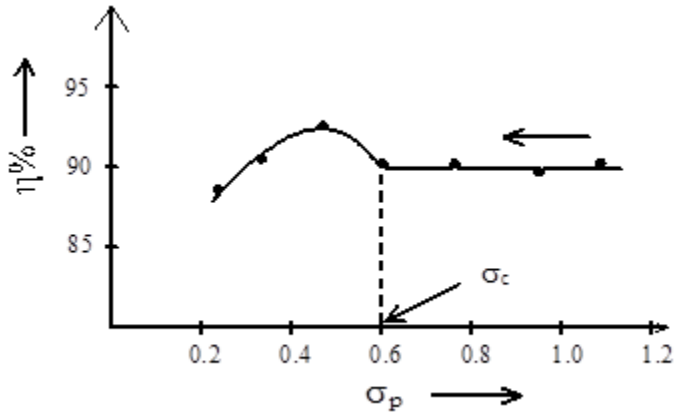

Figure 2 Variation of efficiency with respect to cavitation factor (σ)

The cavitation may occur in high speed hydraulic machines such as turbines, pumps, marine propellers and in hydraulic structures such as spillways and openings of high dams. It may also occur in certain portions of the pipeline and some devices used for flow measurement. It may be noted that the damage to the solid boundary occurs at a point of bubble collapse and not in the region of minimum pressure. So since the collapse takes place in the region of high pressure zone, the damage, therefore, lies downstream of the point of minimum pressure. It may, therefore, be seen that the formation of vapor bubbles, is not damaging in itself, but represent a source associated with severe damage of boundary with considerable vibrations and noise.

Bernoulli's equation expressed as energy per unit volume is given by

$$(\rho * V^2 / 2) + p + \gamma Z = Ev \quad (1)$$

The pressure at a point is

$$p = Ev - (\rho * V^2 / 2) - \gamma Z \quad (2)$$

The total energy per unit volume E_v is a constant along a streamline in a rotational flow and at all points in an irrotational flow. The pressure p at a point, then, depends upon the velocity and datum head. The pressure may get reduced either by increased velocity or on account of higher elevation head or due combination of both. At certain regions in the flow, these variables may be so combined as to reduce the pressure to its vapor pressure value. Once this pressure is obtained, the cavitation is imminent. Engineers are, therefore, required to design and operate the hydraulic machines and structures in such a way that the possibility of occurrence of cavitation is ruled out. While designing, we must ensure that nowhere in the flow, pressure falls to such a low value as the vapor pressure of the liquid at the prevailing temperature. In the case of water, the absolute pressure head should not be allowed to fall below 2.5m in order to prevent cavitation.

2. CAVITATION AT RUNNER VANE MOVING ZONE

Bulb turbine units are used in the run-of-river hydroelectric power plants for low head ranges. The runner vanes operations and guide vanes operations are synchronized to

produce the maximum turbine efficiency for a given head and discharge. The higher specific speeds in the bulb turbines make the full advantage of the concept of total energy utilization to result the maximum efficiency. The aim is to produce higher efficiencies over a lower net head range. This is especially critical in the run-of-the river plants where dry seasons contribute too much of the annual operating period. The upstream river geometry significantly influences the flow pattern into the turbine. Poor orientation of the turbine inlet to the direction of flow in the river results in flow separation at the intake. Eddies and vortices form during the draw at of water, which adversely affect the turbine performances. A straight conical diffuser draft tube with a transition section from circular to rectangular cross section is utilized in these turbines.

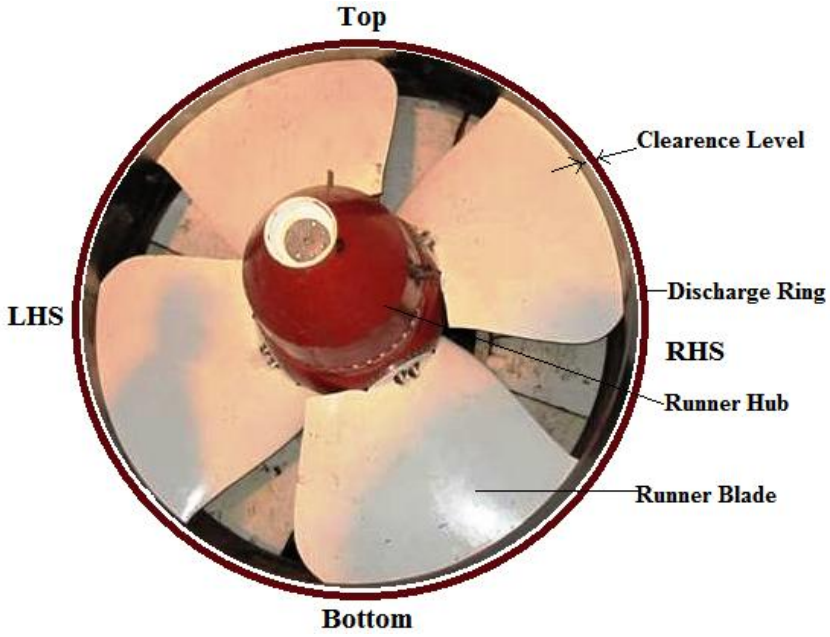

Figure 3 Runner vane assembly inside the discharge ring

The cavitation pitting is seen in the flow area of are in the discharge ring. The discharge ring assembly houses the runner vane assembly shown in Figure 3. The discharge ring connects the distributor cone assembly and draft tube. The discharge ring assembly has four numbers of 20 mm copper pipes at the top half of the water spraying between the rotating runner vane and the discharge ring during condenser operations. As the velocity of the water at the exit of the runner vanes is high as 9.37 m/s, the water boils inside the discharge ring due to the lowest vapor pressure of flowing water. The vapor pockets, thus formed at the exit of the runner vane, moves to a region of higher pressure inside the discharge ring where it collapses suddenly and causes noise, vibration and pitting of the discharge ring. As the growth of bubbles and their collapse take place at a high speed, the damage to the discharge ring is largely due to fatigue, and the damaged metal surface appears with numerous drilled holes of different diameters varying from 3 mm to 6 mm with different depth of penetration from 6 mm to 10 mm.

3 CAVITATION PITTING AND ITS EFFECT ON DISCHARGE RING

The discharge ring is subjected to a higher-pressure force due to cavitation that acts as repeated hammer blows. Whenever these forces are less than the elastic limit of the material of the discharge ring, there is no deformation. But when the quantum of the cavitation force acting on the discharge ring is higher than the elastic limit of the material, then the deformation of discharge ring is permanent. It has been observed, during the annual maintenance that the discharge ring which is deformed and gets back to the original shape when same is dismantled and reassembled. But the cavitation forces acted year, after year has stressed the discharge ring beyond its elastic limit. Hence the discharging has to be replaced with a new at with a higher cost with a huge loss of revenue to the power utility services.

4 RUNNER VANE CLEARANCE

The cavitation and water hammer forces are acting in the discharge ring. The cavitation forces are emerging out due to low pressure region created inside the discharge ring at small guide vane openings. The water hammer forces were acting in the discharge ring at the time of shutdown of the machine due to the deep setting of the turbine runner. Whenever the total forces are within the elastic limits of the discharge ring, the deformation is elastic. But when the forces exceed the elastic limit of the discharge ring the deformation of the discharge ring is in the plastic region, and the deformation is permanent. This was confirmed while the repairing and rectification work carried out in the powerhouse and the results are shown in Table 1 and Figure 4

Table 1 Different Clearance levels with respect to no of hours working

Number of Hours Worked in 1000	Top Clearance measured in mm	Bottom Clearance measured in mm	L.H.S Clearance measured in mm	R.H.S Clearance measured in mm
0	3.75	2.85	2.70	2.65
0.9	3.75	2.85	2.70	2.60
2.1	3.75	2.85	2.70	2.55
7.5	3.75	2.85	2.70	2.50
12	3.75	2.85	2.70	2.45
16.4	3.75	2.85	2.70	2.40
44.03	4.60	3.30	1.20	1.50
49	5.75	3.65	1.20	1.50
52.5	5.75	3.85	1.20	1.20
54.6	5.75	3.85	1.20	1.15
55	5.75	3.85	1.20	1.15

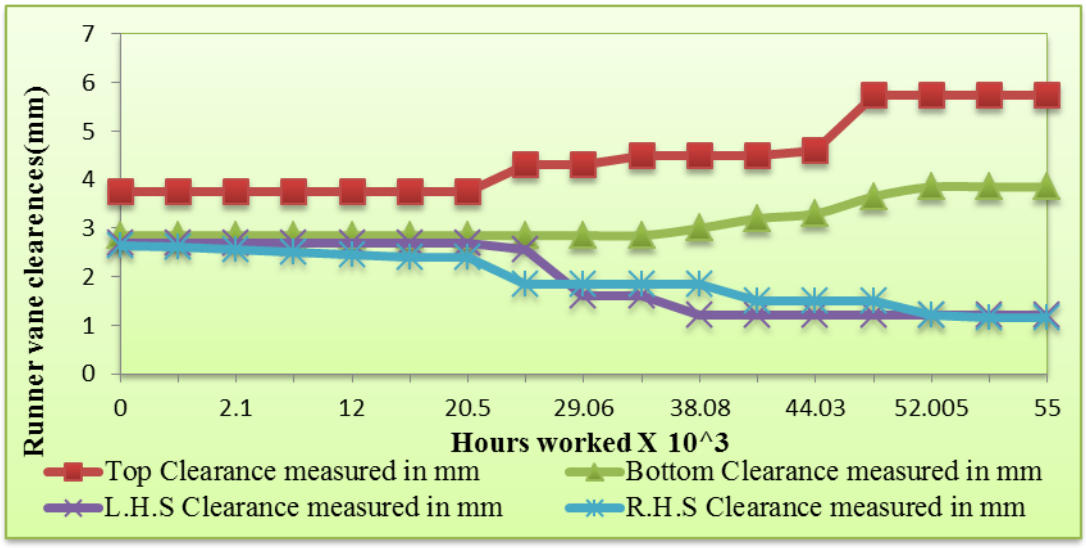

Figure 4 Runner vane clearance levels of new machine

With the help of Microsoft Excel curve fitting software using Least Square method. The equation for the runner vane Top clearance for condition-1 has been derived as $T = 0.0002d^2 + 0.0825d + 3.275$, where T = Clearance in mm in the Top direction. d = No. of hours worked in 1000. The curve fitting equation for the Top clearance for condition-2 has been derived as $T_1 = -0.0030d_1^2 - 0.165d_1 + 3.607$, where T_1 = Clearance in mm in the Top direction and d_1 = No. of hours worked in 1000. The clearances obtained by solving these curve fitting equations are compared with the measured clearances listed in Table 2 and are shown in Figure 5

Table 2 Discharge ring top clearance levels

Number of Hours Worked in 1000	Top Clearance Calculated Using governing Equation	Top Clearance measured in mm
0.9	3.7688	3.75
2.1	3.7505	3.75
7.05	3.7036	3.75
12	3.7025	3.75
16.4	3.7405	3.75
20.5	3.8088	3.75
24.7	3.9116	3.75
40	4.5672	4.50
44.03	4.8133	4.50
49	5.159	4.60
52.05	5.4000	5.75
54.06	5.3906	5.75
55	5.6384	5.75

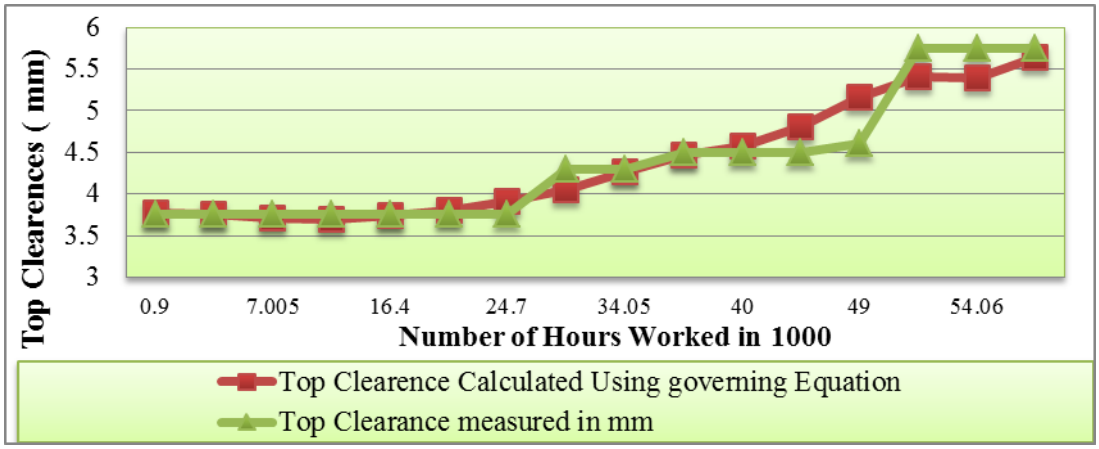

Figure 5 Runner vane clearance at top

Similarly by using Microsoft Excel curve fitting software the equation for the runner vane Bottom clearance for condition-1 has been derived as $B = 0.0015d^2 + 0.0765d + 3.275$, where B = Clearance in mm in the Bottom direction. d = No. of hours worked in 1000. The curve fitting equation for the Bottom clearance for condition-2 has been derived as $B_1 = -0.0020d_1^2 + 0.1133\ d_1 + 3.747$, where B_1 = Clearance in mm in the Bottom direction and d_1 = No. of hours worked in 1000. The clearances obtained by solving these curve fitting equations are compared with the measured clearances and are shown in Table 3 and in Figure 6.

Table 3 Discharge ring bottom clearance levels

Number of Hours Worked in 1000	Bottom Clearance measured in mm	Bottom Clearance Calculated Using governing Equation
0.9	2.85	2.8463
2.1	2.85	2.8173
7.05	2.85	2.724
12	2.85	2.6706
16.4	2.85	2.6585
20.5	2.85	2.6766
24.7	2.85	2.7245
38.08	3.00	3.0755
40	3.20	3.1507
44.03	3.30	3.3286
49	3.65	3.5858
52.05	3.85	3.7615
54.06	3.85	3.8904
55	3.85	3.9517

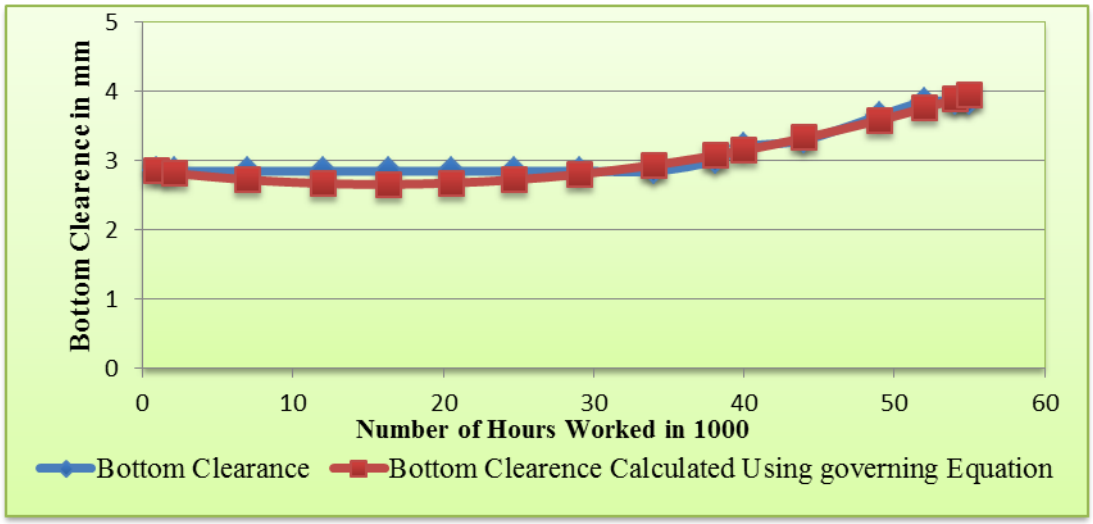

Figure 6 Runner vane clearance at bottom

The equation for the runner vane LHS clearance for condition-1 has been derived using Microsoft Excel curve fitting software as $L = -0.00275d^2-0.0305d + 2.8015$, where L = Clearance in mm in the LHS direction. d= No. of hours worked in 1000. The curve fitting equation for the LHS clearance for condition-2 has been derived as $L_1 = 0.0020\ d_1^2 - 0.1301\ d_1 + 3.0945$, where L_1= Clearance in mm in the LHS direction and d_1= No. of hours worked in 1000. The clearances obtained by solving these curve fitting equations are compared with the measured clearances and are shown in Figure 7 and listed in Table 4

Table 4 Discharge ring L.H.S clearance levels

Number of Hours Worked in 1000	L.H.S Clearance Measured	Left Clearance Calculated Using governing Equation
0.9	2.70	2.7611
2.1	2.70	2.734
7.05	2.70	2.618
12	2.70	2.4913
16.4	2.70	2.3726
20.5	2.70	2.2559
24.7	2.70	2.13
40	1.2	1.62
44.03	1.2	1.47
49	1.20	1.2847
52.05	1.20	1.1659
54.06	1.20	1.0829
55	1.20	1.0445

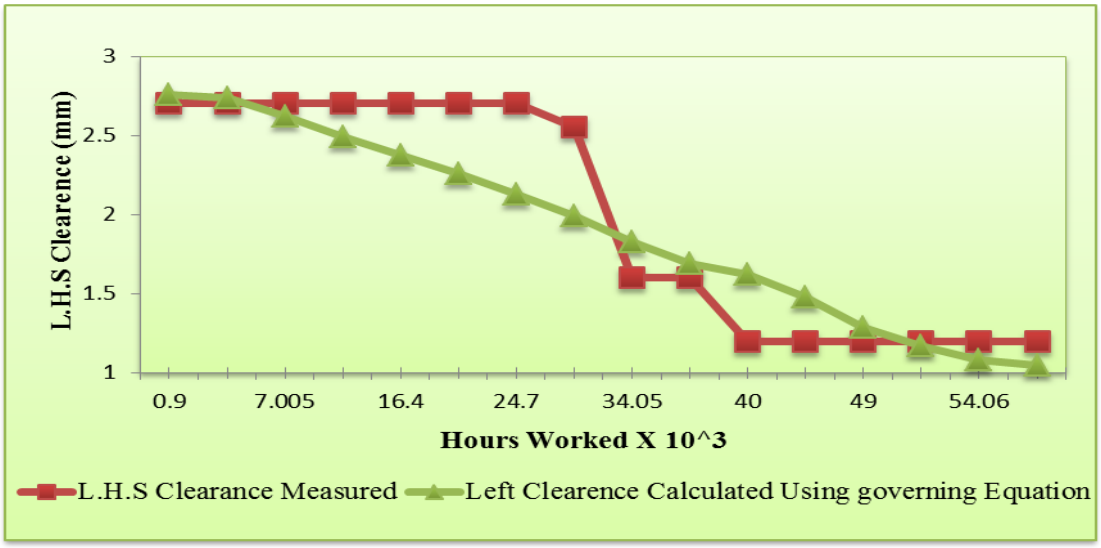

Figure 7 Runner vane clearances at left hand side

The equation for the runner vane RHS clearance for condition-1 has been derived using Microsoft Excel curve fitting software as $R = -0.0030d^2 - 0.0300d + 2.8016$, where R = Clearance in mm in the RHS direction. d = No. of hours worked in 1000. The curve fitting equation for the RHS clearance for condition-2 has been derived as $R_1 = 0.0015d_1^2 - 0.110\ d_1 + 2.8975$, where R_1 = Clearance in mm in the RHS direction and d_1 = No. of hours worked in 1000. The clearances obtained by solving these curve fitting equations are compared with the measured clearances and are shown in Table 5, Figure 8.

Table 5 Discharge ring RHS clearance levels

Number of Hours Worked in 1000	R.H.S Clearance measured in mm	R.H.S clearances Calculated Using governing Equation
0.9	2.60	2.645
2.1	2.55	2.6139
7.05	2.50	2.4852
12	2.45	2.3519
16.4	2.40	2.2326
20.5	2.40	2.1199
38.08	1.85	1.6195
40	1.50	1.5631
44.03	1.50	1.4438
49	1.50	1.2947
52.05	1.20	1.2034
54.06	1.15	1.1405
55	1.15	1.1116

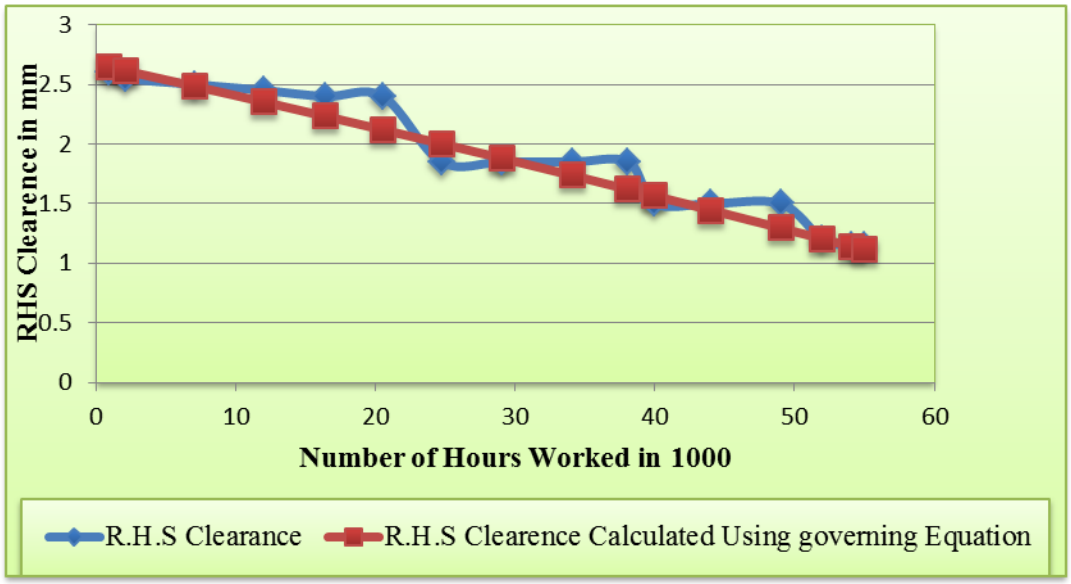

Figure 8 Runner vane clearance at right hand side

5 PRESSURE VARIATION INSIDE THE DISCHARGE RING

A flow for which the streamlines are concentric circles is called a vortex. Fluid dynamics have identified two types of vortices that can be easily described mathematically. One is called the forced vortex in which the velocity increases linearly from the center of rotation. The other type of vortex is the free, or potential, vortex. In a free vortex, the product of the velocity at a point and the radial distance from the vortex, center to that point is a constant (Vr = C). Flow patterns that are developed by – flow inside the discharge ring is an irrotational flow and this flow is closely approximated. The flow of water in this region where the streamlines are converging usually approximates the irrotational flow quite closely. However, in regions where boundaries turn away from the flow so as to cause the streamlines to diverge, the flow usually, separates, from the discharge ring and a recirculation pattern are generated in this region. This phenomenon is called separation. In the region between the high – velocity flow outside the zone of separation and the low velocity zone inside it, vortices are formed. These vortices are often called eddies. These vortices or eddies lead to the phenomenon called turbulence.

As the flow passages in the bulb turbines are converging, the flow is irrotational. Hence Bernoulli's equation is used to obtain the pressure variation between points in the flow field, including points adjacent to the boundaries. Bernoulli's equation between the reference point and any other point is

$$\frac{p}{\gamma}+\frac{V^2}{2g}+z=\frac{p_0}{\gamma}+\frac{V_0^2}{2g}+z_0 \qquad (3)$$

where P_0, V_0, and Z_0 are pressure, velocity, and elevation, respectively, at the reference point; and p, V, and z are pressure, velocity and elevation at any other given point.

By simple rearrangement, Equation (3) is written as

$$p - p_0 = \gamma(z_0 - z) + \frac{\rho}{2}\left(V_0^2 - V^2\right) \tag{4}$$

Equation expresses the pressure change in terms of the change in hydrostatic pressure (the first term on the right) and the change in kinetic pressure (the second term on the right). Thus the dynamic effect is given by

$$\left(\frac{p}{\gamma} + z\right) - \left(\frac{p_0}{\gamma} + z_0\right) = \frac{\rho}{2\gamma}\left(V_0^2 - V^2\right) \tag{5}$$

Equation (4) expresses the change in piezometric head as a function of the difference in the velocities squared, and it reduced to

$$h - h_0 = \frac{V_0^2 - V^2}{2g} \tag{6}$$

where h is the piezometric head at a given point, and h_0 is the piezometric head at the reference point.

Hence, $$\frac{h - h_0}{V_0^2 / 2g} = 1 - \left(\frac{V}{V_0}\right)^2 \tag{7}$$

$$\frac{P - P_0}{\rho V_0^2 / 2} = 1 - \left(\frac{V}{V_0}\right)^2 \tag{8}$$

Because the velocity is inversely proportional to the cross-sectional area through which flow occurs in the flow passage (that is, $V/V_0 = A_0/A$), we can express the relative pressure distribution or piezometric – head distribution in terms of the dimensions of the flow passage. For two-dimensional flow, the streamline spacing is directly proportional to the flow area. Thus we have $V/V_0 = n_0/n$ for the relationship between the relative-velocity distribution and the relative-stream-line spacing. Here n is the distance between two adjacent streamlines measured along the line (possibly curved) perpendicular to both streamlines. As the flow pattern in a bulb turbine is symmetrical with either a vertical or the horizontal axis through the center of runner boss of bulb turbine, the pressure distribution on the surface of the runner boss, obtained by application of Bernoulli's equation, is also symmetrical. The relative pressure C_p is plotted outward (negative) or inward (positive) from the surface of the runner boss, depending on the sign of the relative pressure and line normal to the surface of the cylinder. It should also be noted that p_0 and V_0 are the pressure and velocity of the free stream far upstream or downstream of the body.

The turbines at a particular powerhouse are subjected to a maximum internal water pressure and water hammer forces. These forces are compared to other units in other power houses. The discharge rings of these units are deformed. The discharge rings of the other units are also in strained. The internal pressure developed during the water flow and the water hammer pressure during shutdown of the machine are added to the cavitation pressure forces inside the discharge ring of these bulb turbines. Whenever, all the three forces acting inside the discharge ring exceeds the yield stress of the material, the discharge ring is likely to deform.

6 GUIDE VANE CLEARANCE

The cavitation and water hammer forces act inside the outer distributor cone and inner distributor cone assembly. The cavitation forces are due to low pressure region created during low guide vane openings inside the distributor cone assembly. The water hammer forces act on the guide vane assembly at the time of shutdown of the machine. Whenever the total forces are within the elastic limits of the guide vane assembly, the deformation of the distributor cone is elastic. But when the forces exceed the elastic limit of the distributor cone the deformation is permanent. This has been confirmed during the repairing work carried out on the Power House.

The equation for the guide vane top clearance for condition-1 has been derived using Microsoft Excel curve fitting software as $T_2 = -0.0003d_1^2 + 0.0675d_1 + 2.2652$, where T_2 = Clearance in mm in the Top direction.d_1 = No. of hours worked in 1000. The equation for the Top clearance for condition-2 has been derived as $T_{21} = -0.0025d_1^2 + 0.0953d_1 + 2.2501$, where T_{21}= Clearance in mm in the Top direction and d_1 = No. of hours worked in 1000. The clearances obtained by solving these equations are compared with the measured clearances and are shown in Table 6 and Figure 9.

Table 6 Clearance levels measured in top of the discharge ring

Number of Hours Worked in 1000	Top Clearance measured in the new machine (condition-1)	Curve fitted for condition1	Top Clearance measured in the same machine after reconditioning (condition-2)	Curve Fitted for condition 2
0	2.20	2.2652	2.20	2.2501
3	2.50	2.5304	2.60	2.5913
6	2.70	2.7860	2.90	2.8525
9	3.00	3.0320	3.00	3.0337
12	3.20	3.2684	3.10	3.1349
15	3.50	3.4952	3.20	3.1561
18	3.70	3.7124	3.10	3.0973
20	4.00	3.9200	3.00	2.9585

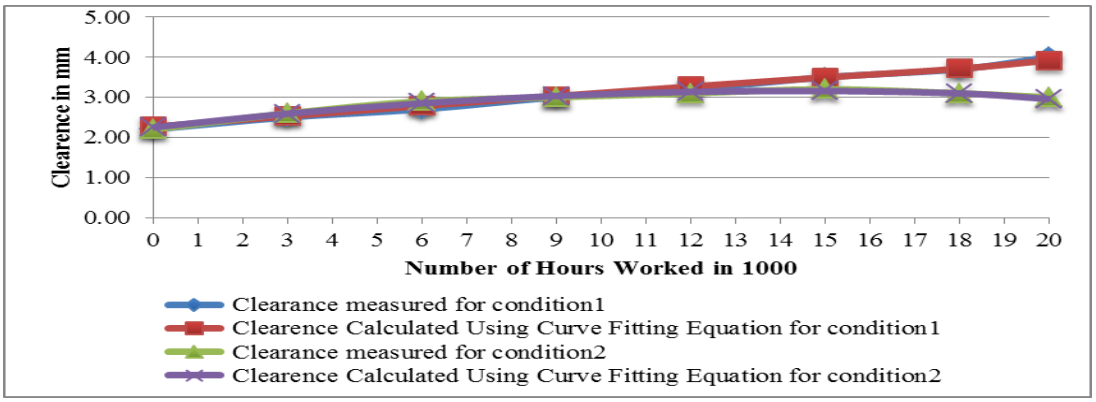

Figure 9 Guide vane clearances at top

The equation for the guide vane bottom clearance for condition-1 has been derived using Microsoft Excel curve fitting software as $B_2 = -0.0024d_1^2 + 0.1320d_1 + 2.1686$, where B_2= Clearance in mm in the bottom direction. d_1 = No. of hours worked in 1000. The equation for the bottom clearance for condition-2 has been derived as $B_{2\,1} = -0.0015d_1^2 + 0.0786d_1 + 3.8531$, where $B_{2\,1}$ = Clearance in mm in the bottom direction and d_1 = No. of hours worked in 1000. The clearances obtained by solving these curve-fitting equations are compared with the measured clearances and are shown in Table 7 and Figure 10.

Table 7 Clearance levels measured in bottom of the discharge ring

number of hours worked in 1000	bottom clearance (condition-1)	curve fitted for condition 1	bottom clearance condition-2	curve fitted for condition 2
0	2.30	2.2982	3.90	3.9302
3	2.70	2.6582	4.00	4.1435
6	3.00	3.0710	4.40	4.3859
9	3.40	3.4070	4.50	4.5803
12	3.60	3.6662	4.70	4.7267
15	3.80	3.8486	4.80	4.8251
18	3.90	3.9542	4.90	4.8755
20	4.00	3.9830	4.95	4.8779

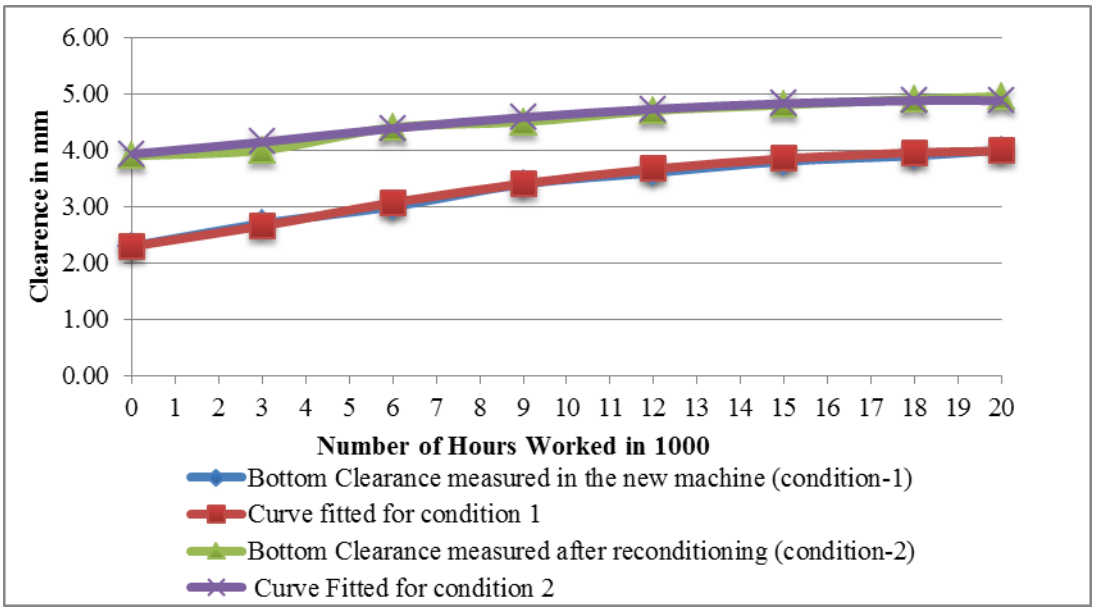

Figure 10 Guide vane clearances at bottom

The equation for the guide vane LHS clearance for condition-1 has been derived using Microsoft Excel curve fitting software as $L_2 = -0.0028d_1^2 + 0.0090d_1 +$

2.3947, where L_2 = Clearance in mm in the LHS direction.d_1 = No. of hours worked in 1000. The equation for the LHS clearance for condition-2 has been derived as $L_{21} = 0.0017d_1^2 - 0.0761d_1 + 1.2634$, where L_{21} = Clearance in mm in the LHS direction and d_1 = No. of hours worked in 1000. The clearances obtained by solving these curve-fitting equations are compared with the measured clearances and are shown in Table 8 and Figure 11.

Table 8 Clearance levels measured in LHS of the discharge ring

Number of Hours Worked in 1000	LHS Clearance (condition-1)	Curve fitted for condition 1	LHS Clearance (condition-2)	Curve Fitted for condition 2
0	2.40	2.3947	1.25	1.2634
3	2.35	2.3859	1.00	0.9862
6	2.30	2.2875	0.75	0.7634
9	2.00	2.0995	0.60	0.5950
12	1.80	1.8219	0.50	0.4810
15	1.40	1.4547	0.42	0.4214
18	1.00	0.9979	0.41	0.4162
20	0.50	0.4515	0.45	0.4654

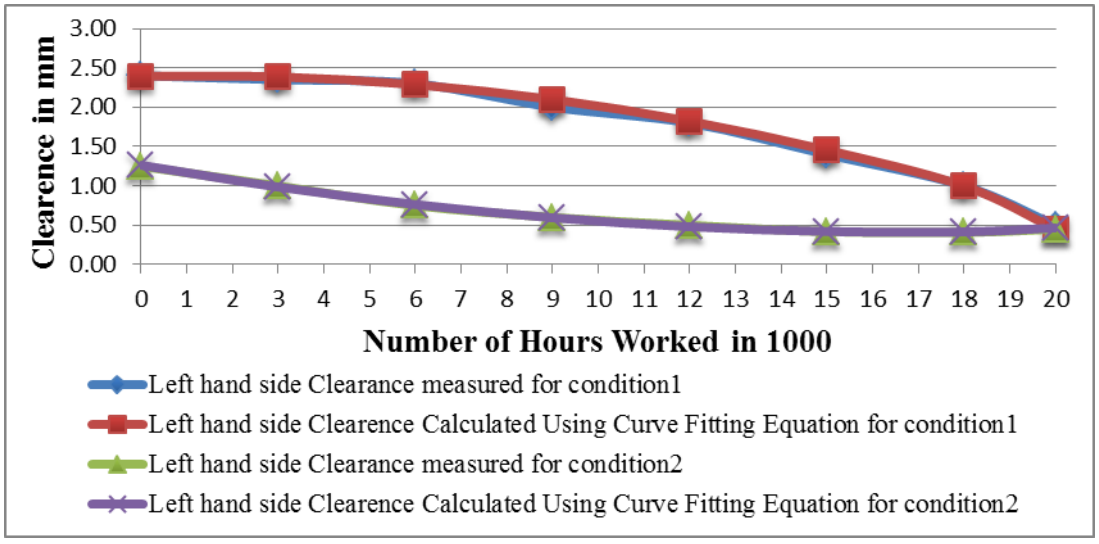

Figure 11 Guide vane clearance at left hand side (LHS)

The equation for the guide vane RHS clearance for condition-1 has been derived using Microsoft Excel curve fitting software as $R_2 = -0.0035d_1^2 + 0.0271d_1 + 2.3411$, where R_2 = Clearance in mm in the RHS direction.d_1 = No. of hours worked in 1000. The equation for the RHS clearance for condition-2 has been derived as $R_{21} = 0.0010d_1^2 - 0.0492d_1 + 1.7595$, where R_{21} = Clearance in mm in the RHS direction and d_1 = No. of hours worked in 1000. The clearances obtained by solving these

curve-fitting equations are compared with the measured clearances and are shown in Table 9 and Figure 12.

Table 9 Clearance levels measured in RHS of the discharge ring

Number of Hours Worked in 1000	RHS Clearance (condition-1)	Curve fitted for condition 1	RHS Clearance measured in the same machine after reconditioning	Curve Fitted for condition 2
0	2.40	2.3647	1.80	1.7595
3	2.38	2.3935	1.60	1.5787
6	2.35	2.3339	1.40	1.4299
9	2.20	2.1623	1.30	1.3131
12	1.80	1.8787	1.20	1.2283
15	1.50	1.4831	1.15	1.1755
18	1.00	0.9755	1.12	1.1547
20	0.40	0.3559	1.15	1.1659

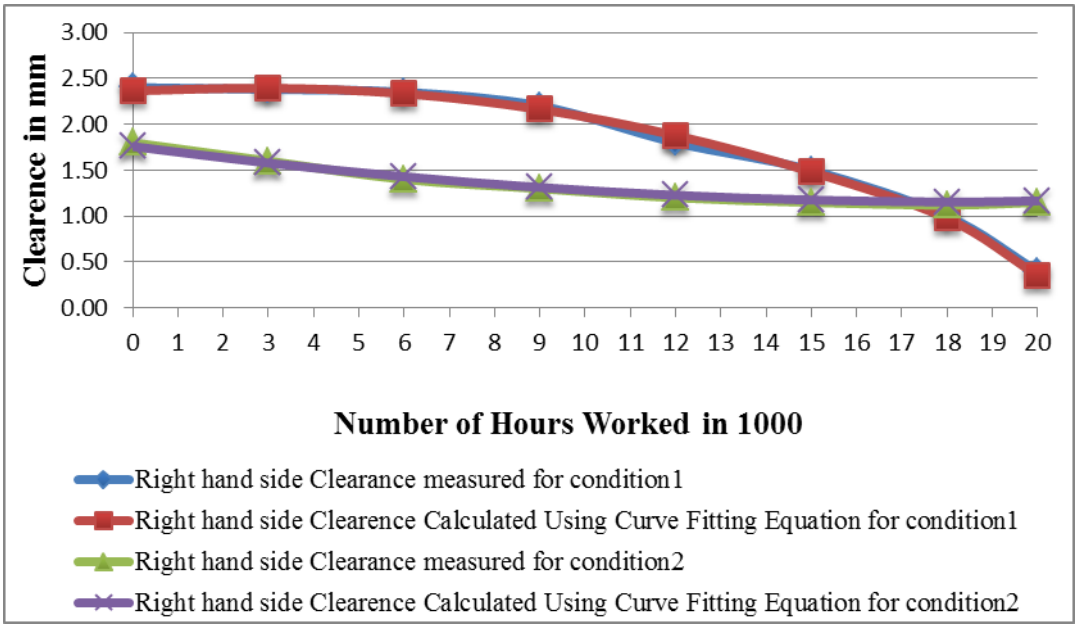

Figure 12 Guide vane clearance at right hand side (RHS)

7 RESULTS AND DISCUSSION

After the operation of about 55,000 hours for the new machine and 20,000 hours, it is found in power house that distributor cone assemblies have been shattered with a very heavy hydraulic and cavitation forces. Distortion has been observed in the contact and moving area of guide vanes assembled between outer and inner distributor cones. The moving clearance for the 4th guide vane has increased to a maximum of 5.8 mm from

a design value of 2 mm. Thus the top portion of the outer distributor cone has lifted up by 3.8 mm.

Similarly the clearance at 12^{th} and 13^{th} guide vanes are also increased to 5.1 mm from the design value of 1.8 mm and showed a distortion in the bottom side of the distributor cone assembly, and has been pulled downwards by 3.3 mm. The clearances at the left side guide vanes 8 and 9 have reduced to 0.02 mm from the design value of 2.7 mm which showed a contraction of 2.68 mm. Similarly, a minimum clearance of 0.02 mm has been recorded at guide vanes 12 and 13 on the right side of the assembly and here also a contraction about 2.88 mm has been noticed. Thus the entire distributor cone assembly has become in distorted condition. The top and bottom portions have elongated by 3 to 5 mm, and the side portions have contracted by 2.8 mm from the design values. Another major problem noticed is the, wide openings between the guide vanes at fully closed condition. These clearances are supposed to be zero at this position but have increased abnormally to a maximum value of 14.5 mm at the guide vanes 6, 7, 14 and 15. The contact clearances at guide vanes 9 to 11 at right hand side, and 2 to 4 at left hand side have increased from 0 to13 mm which impose a very dangerous condition for a hydro turbine. The machine could not be stopped by applying brake, due to heavy water leakage passing through these guide vanes.

8 CONCLUSION

The turbine manufacturer recommended that the unit should not be run below 50% wicket gate (guide vane) due to excessive cavitation levels. This warning has been confirmed by measurements taken on the bulb turbines by this experiment also. It has been also found that the turbine experienced higher cavitation acoustic emission levels when the guide vane opening is less than 50%.

It has been found that energy modulation levels at the blade passing frequency for the hydro turbine indicate the reasons for severe erosive cavitation occurring when the hydro units are operated at guide vane openings below 50 percent and above 90 percent. Cavitation damage is minimal at around 60 percent guide vane opening. This is confirmed in this study by the vibration and noise measurements taken on the discharge ring for different guide vane openings from 30 to 90%. In this study, it has been found that the tail race water level has influenced the cavitation occurrence in the bulb turbines which are located at different places with different suction head (H_s).

The deformation of discharge ring is calculated and correlated with the hours of operation. This is a very useful method to predict the life of discharge ring and for scheduling the repairs and replacement at appropriate time on bulb turbines. These findings also help the designer to take care of cavitation phenomenon and deformation of discharge ring by using these equations for bulb turbines.

It has been found out that there are three distinct regions in our study namely

(i) minimum pressure region upstream of separation at the exit of the guide vane
(ii) the separation region between guide vane and runner vane at the entry of the runner vane and

(iii) the reattachment region in the draft tube. It has been found that the bubble growth in the separated region has played an important role in cavitation inception at the exit of guide vanes.

It has been confirmed that, for the cavitation erosion phenomenon, the pressure waves-impact seems to be the mechanism responsible for the damage observed. The study confirms that the water hammer forces are caused by rapid flow cut-off. The backwater hammer effects are also realized, in addition to cavitation forces, Results of the investigation highlighted these problems that are to be taken into account during the process of design of hydropower plants with bulb turbines.

This study gives correlations between the distortion of outer distributor cone and number of hours worked in the form of equations as indicated earlier. The same type of distortion and cavitation pitting are also observed again after reconditioning within a short period, which is also given by the same type of equations for top, bottom, left hand side and right hand sides of the assembly.

REFERENCES

[1]. Abbas, M, Khan, SM & Ali, N 2011, 'Fuzzy Logic Based Hydro-Electric Power Dam Control System', International Journal of Scientific & Engineering Research, vol. 2, no. 6,pp. 1-8.

[2]. Agostino, L & Burzagli, F 2000, 'On the Stability of Parallel Bubbly Cavitating Flow', Journal Fluid Engineering, vol. 122, no.3, pp. 471-480.

[3]. Ahmad, I & Asif, S 2007, 'Elements of an Effective Repair Program for Cavitation Damages in Hydraulic Turbines', Information Technology Journal, vol.6, no.8, pp.1276-1281.

[4]. Akesson, H & Sigfridsson, A 2010, 'Vibration Absorption And Health Monitoring In A Hydroelectric Power Plant', Proceedings of International Congress on Sound and Vibration, Cairo, Egypt, pp.1-8.

[5]. Arb, C, Avellan, F & Henry, P 1994, 'Mechanism of the Efficiency Drop due to Traveling Bubble Cavitation', XVII IAHR Symposium Beiging, China, pp. 11-22.

[6]. Arndt, REA & Maines, BH 2000, 'Nucleation and bubble dynamics in vertical flows', Journal of Fluid Engineering, vol. 122, no.3,pp. 488-493.

[7]. Auria, FD, Agostino, LD & Brennen, CE 1996, 'Dynamic Response of Ducted Bubbly Flow to Turbo Machinery Induced Perturbations, Journal of Fluids Engineering, vol.118, no.3, pp. 595-601.

[8]. Bajic, B 2001,'Intelligent Cavitation Diagnostics and Monitoring' International Water Power & Dam Construction,vol.54, no.5,pp.33-37.

[9]. Balachandar, R & Ramamoorthy, A S 1999, 'Pressure Distribution in Cavitating Circular Cylinder Wakes', Journal of Engineering Mechanics, vol.125, no.3, pp. 356-358.

[10]. Bechtel, TB 2003, 'Laminar Pipeline Flow of Waste Water Sludge: Computational Fluid Dynamics Approach', Journal of Hydraulic Engineering , vol.132, no.2, pp. 153-158.

[11]. Bedout, DJM, Frenchek, MA & Mongeau, L 1997, 'Self Tuning Helmholtz Resonators', Journal of Sound and Vibration, vol.125, pp.192-197.

[12]. Berchiche, N, Franc, J P & Michel, J M 2002, 'A Cavitation Erosion Model for Ductile Materials', Journal of Fluid Engineering, vol. 124, no.3,pp. 601–606.

[13]. Branko, B & Andreas, K 1996, 'Spectrum Normalization Method in Vibro-Acoustical Diagnostic Measurements of Hydro Turbine Cavitation', ASME Journal of Fluids Engineering, vol.118, no.4,pp. 756-761.

[14]. Brennan, MJ 1997, 'Vibration Control Using a Tunable Vibration Neutralizer', Pro Inst. Mech. Eng. Part C, Journal of Mechanical Engineering Science, vol. 221, Part C, pp. 91-108.

[15]. Brennan, MJ 1998, 'Actuators for Active Vibration Control – Tunable Resonant Devices', 4th Euro Conference on Smart Structures and Materials, pp. 41-48.

[16]. Brunone, B & Morelli, L 1999, 'Automatic Control Value – Induced Transients in Operative Pipe System', Journal of Hydraulic Engineering, vol. 125, no.5, pp. 534-542.

[17]. Chen, K & Koopmann, GH 2002, 'Active Control of Low Frequency Sound Radiation From Vibrating Panel Using Planner Sound Sources', Journal of Vibration and Acoustics, vol. 124, no.1, pp.2-9.

[18]. Cheng, Y & Heister, SD 1996, 'Modeling Hydrodynamic Nonequilibrium in Cavitating Flows', Journal of Fluids Engineering, vol. 118, no.1, pp. 172-178.

[19]. Cojocaru, V & Balint, D 2011, 'Numerical Investigations of Flow on the Kaplan Turbine Runner Blade Anticavitation Lip with Modified Cross Section', Recent Researches in Mechanics, vol.37, pp. 215-218.

[20]. Corr, LR & Clark, WW 2003, 'A Novel Semi – Active Multi Model Vibration Control Law for a Piezometric Actuator', Journal of Vibration and Acoustics, vol. 125, no.2, pp. 214-222.

[21]. Croll, JGA 2001, 'Bucking Cylindrical Tunnel Lines', Journal of Engineering Mechanics, vol. 127,no.4, pp. 333-341.

[22]. De-souza, AC 2008, 'Assessment and statistics of brazilian hydroelectric power plants: dam areas versus installed and firm power'. Renewable and sustainable energy reviews, vol.12, no.7, pp. 1843-1863.

[23]. Doering, JC & Gawne, KD 1998,'Developing a Traversing Acoustic Discharge Measurement Technique for the Performance Testing of Low Head Hydro Electric Turbines', Canadian Journal of Civil Engineering, vol. 24, no.4, pp. 777-788.

[24]. Doering, JC & Hans, P D 2001, 'Turbine Discharge Measurement by the Velocity Area Method' Journal of Hydraulic Engineering, vol.127, no.9, pp. 747-752.

[25]. Dugue, C, Fruman, DH, Billard, JY & Cerrutti, P 1992,'Dynamic Criterion for Cavitation of Bubbles', Journal of Fluids Engineering, vol. 114, no.2, pp.250-254.

[26]. Espitia, LA & Toro, A 2010, 'Cavitation resistance, microstructure and surface topography of materials used for hydraulic components', Tribology international, vol. 43, pp. 2037-2045.

[27]. Falvey, HT & Weldon, JH 2002, 'Case Study: Dillon-Dam Trash-Rach Damage', Journal of Hydraulic Engineering, vol.128, no.2, pp. 144- 150.

[28]. Fan, D & Jijsseling, A 1992, 'Fluid Structure Interaction with Cavitation in Transient Pipe Flows', Journal of Fluids Engineering, vol. 114, no.2, pp. 268-274.

[29]. Farrell, KJ 2003, 'Eulerian / Lagrangian Analysis for the Prediction of Cavitation Inception', Journal of Fluids Engineering, vol. 125, no.1, pp. 46-52.

[30]. Flamos 2011, 'Hydro Energy: Techno economic and Social Aspects Within New Climate Regime'. International Journal of Renewable Energy Technology, vol.2, no.1, pp.32-62.